



Origins of Soft-Sediment Deformation Structures from the Batang Paleo-dammed Lakes in the Upper Jinsha River, SE Tibetan Plateau

Yongbo Teng¹, Jian Chen^{1*}, Zhijiu Cui², Weichao Li³ and Yan Li¹

¹School of Engineering and Technology, China University of Geosciences, Beijing, China

²College of Urban and Environmental Sciences, Peking University, Beijing, China

³State Key Laboratory of Simulation and Regulation of Water Cycle in River Basin, China Institute of Water Resources and Hydropower Research, Beijing, China

Abstract

Multiple levels of preserved soft-sediment deformation structures occur in sediments deposited in the paleo-dammed lakes in the Batang-Zhongza reaches of the upper Jinsha River Valley, southeast Tibetan Plateau. These deformation structures include folded layers, convoluted layers, ball-and-pillow structures, recumbent lamination, water-escape structures, and small-scale landslide. Combining the assessments of depositional facies, potential triggers, paleoenvironmental context, we conclude that the probable trigger agents of this deformation were earthquakes, slides, and debris flows. The seismically-induced soft-sediment deformation structures provide new substantial evidence for the existence of active tectonics and paleo-earthquakes in the Batang area since the Holocene.

Keywords: Batang paleo-dammed lake; Soft-sediment deformation; Paleoeearthquake; Jinsha river

Introduction

Soft-sediment deformation (SSD) is deformation that usually occurs rapidly in unconsolidated sediment close to the surface, during or shortly after deposition, and before significant diagenesis [1]. Soft sediment deformation structures (SSDS) are features occurring in unconsolidated sediment. SSD can be induced by many natural processes, including gravity acting, overloading, unequal loading, wave-induced cyclical or impulsive stresses, shear by aqueous or other currents, storms, sudden changes in groundwater level, or earthquakes [2-9]. SSD features are known from a wide variety of depositional environments, both terrestrial: fluvial, aeolian or volcanic [9-11], or marine: shore, turbiditic, subglacial [12-14], but they are particularly well-reported from lacustrine depositional environments [15-31]. The relative abundance of seismites in lacustrine successions is explained by Sims [15] in terms of: (1) the presence of water-saturated sediments; (2) the presence of sediments with high susceptibility to liquefaction; (3) the absence of hydrodynamic and sedimentary processes able to obliterate the products of seismically-induced deformation. Liquefaction and fluidization are two common deformation mechanism for the soft-sediment deformation structures. Liquefaction occurs when grain weight is temporarily transferred to the pore fluid, through either the collapse of a loose grain packing or an increase in pore-fluid pressure [2,21,32]. The likely products are pervasive structures that deform existing stratification [33]. Fluidization occurs when the upward-directed shear of fluid flowing through a porous medium counteracts the grain weight, reducing the material strength [2,9,21,24]. The process may develop new stratification [20].

SSDS such as convolute lamination, load structures, pillar structures, water-escape structures and deformed cross-bedding are common in sands contained lacustrine environments. However, very little published documentation exists for SSD generated in dammed lacustrine settings due to the relatively short life span of dammed lakes. The spatial distribution of SSD features has significant implications for the interpretation of their origins and can help in understanding the evolution of paleo-dammed lakes. On the southeastern margin of the Tibetan Plateau, the erosion rate is high and the mass movement is frequent and young strata are rarely preserved intact, thereby hindering direct studies of paleo-sesimicity by fault outcrops. Therefore, the

recognition of seismically-triggered structures is an important factor in determining earthquake recurrence intervals in paleo-seismic studies [13,22,34]. In this paper we first describe the type and nature of the soft-sediment structures preserved in the Batang paleo-dammed lake sediments. Then we interpret and discuss the mechanisms of their formation. Finally, we present the implications of this evidence for regional tectonics.

Regional Setting

The Batang-Zhongza reaches are located in the upper Jinsha River at the southeastern margin of the Tibetan Plateau (Figure 1a), and are about 90 km in length. The Jinsha River flows through the west side of Batang County from north to south, and mountains have developed along both sides of the river where the valleys are incised deeply. The average elevation of the area is greater than 2200 m; and the river is confined between steep banks (>40°), prone to rock falls, rock slides and small debris flows. Rock slides and debris flows are often seen on steep concave banks. The lithology of the exposed rocks along the valley sides are mainly Mesozoic schist, marble and limestone, granite, as well as other volcanic rocks [7].

The climate in this segment is mainly semi-arid, but changes significantly with height. In the lower valleys the climate is arid and hot. The average precipitation is less than 400 mm/year and the average temperature of the warmest month is 13-16°C. Due to the influence of the southwest monsoon, the rainfall is concentrated within July-September of every year. In Batang, the monthly mean temperature is

***Corresponding author:** Jian Chen, School of Engineering and Technology, China University of Geosciences, 100083, Beijing, China, Tel: +86 10 82321196; E-mail: jianchen@cugb.edu.cn

Received September 06, 2017; **Accepted** September 18, 2017; **Published** September 26, 2017

Citation: Teng Y, Chen J, Cui Z, Li W, Li Y (2017) Origins of Soft-Sediment Deformation Structures from the Batang Paleo-dammed Lakes in the Upper Jinsha River, SE Tibetan Plateau. J Geol Geophys 6: 306. doi: [10.4172/2381-8719.1000306](https://doi.org/10.4172/2381-8719.1000306)

Copyright: © 2017 Teng Y, et al. This is an open-access article distributed under the terms of the Creative Commons Attribution License, which permits unrestricted use, distribution, and reproduction in any medium, provided the original author and source are credited.

3.7°C for January and 19.5°C for July. It is due to this climate that in this area physical weathering is strong and vegetation is poorly developed.

There are two active faults systems which pass through the segment. One is the Batang fault (F1) and the other is the Jinshajiang fault zone (F2). The latter is composed of the Zengziding fault (F2-1), Zigasi-Deeqeen fault (F2-2), Benxie-Dagaiding fault (F2, F3), and Xionsong-Suwanglong fault (F2-F4) (Figure 1a). Among these, the Xionsong-Suwanglong fault (F2-F4) is a major one, which passes through the east side of the Wangdalong - Zhubalong area [8]. The faulted landform and chronology show that the current right-lateral strike-slip rate of the Jinsha River fault zone is 6-7 mm/a, and the vertical rate is estimated at 2-3 mm/a [35].

According to existing historical records, since 1722, seven earthquakes of $M \geq 6$ have occurred in this segment and its adjacent areas [36]. Among them, the strongest earthquake, at $M=7.5$, occurred in 1870.

Sediments Within Paleo-dammed Lakes

Several paleo-dammed lakes occurred as the form of single individual or a series in the Batang-Zhongza reaches of the upper Jinsha River (Figure 1b). Paleo-lake evidences consist of relict barrier bars preceded on their upstream side by lacustrine sediments (from several to tens of metres in thickness) (Figure 2a). The lake sediments occur on the upriver side of relict barrier bar deposits. The thickness of the dammed lake sediments decreases with increasing altitude. The lacustrine sediments are dominantly characterized by clear horizontal bedding, and consist mainly of fine sands, silts, and clays. The results of optical stimulated luminescence (OSL) and ^{14}C dating data show that

these dammed lakes formed during the Holocene [7,19,37]. In addition, soft-sediment deformation structures are found among these paleo-dammed lake sediments (Figure 2b).

Soft-sediment Deformation Structures

The entire lacustrine succession of the upper Jinsha River valley shows many soft-sediment deformation structures at different stratigraphic levels (Table 1). In this paper, the morphologies of the soft-sediment deformation structures were studied in the field through the natural exposure profiles, or the excavation of trenches.

Based on the size and main morphological features, six different types of soft-sediment deformation structures in the dammed lake sediments have been distinguished: 1 - Folded layers, 2 - Convoluted layers, 3 - Ball-and-pillow structures, 4 - Recumbent lamination, 5 - Water escape structures, and 6 - Small-scale landslide.

Folded layers

The folded layers forming the angular unconformity occur near the base of the clayey-silt layers of the lacustrine sediments located around the Temi Village (Figure 3a). Two normal faults occur in the deformed cross-bedding at the lower part of the S section. The deformed clayey-silt layers formed folds on both sides of the fault planes. The faulting has ruptured and slightly displaced the laminated brown clayey-silt (Figure 3b).

Convoluted layers

The convoluted layer occurred in ~40 cm thick horizons at the central part of the profile (Figure 4a), and its overlying clayey silt is

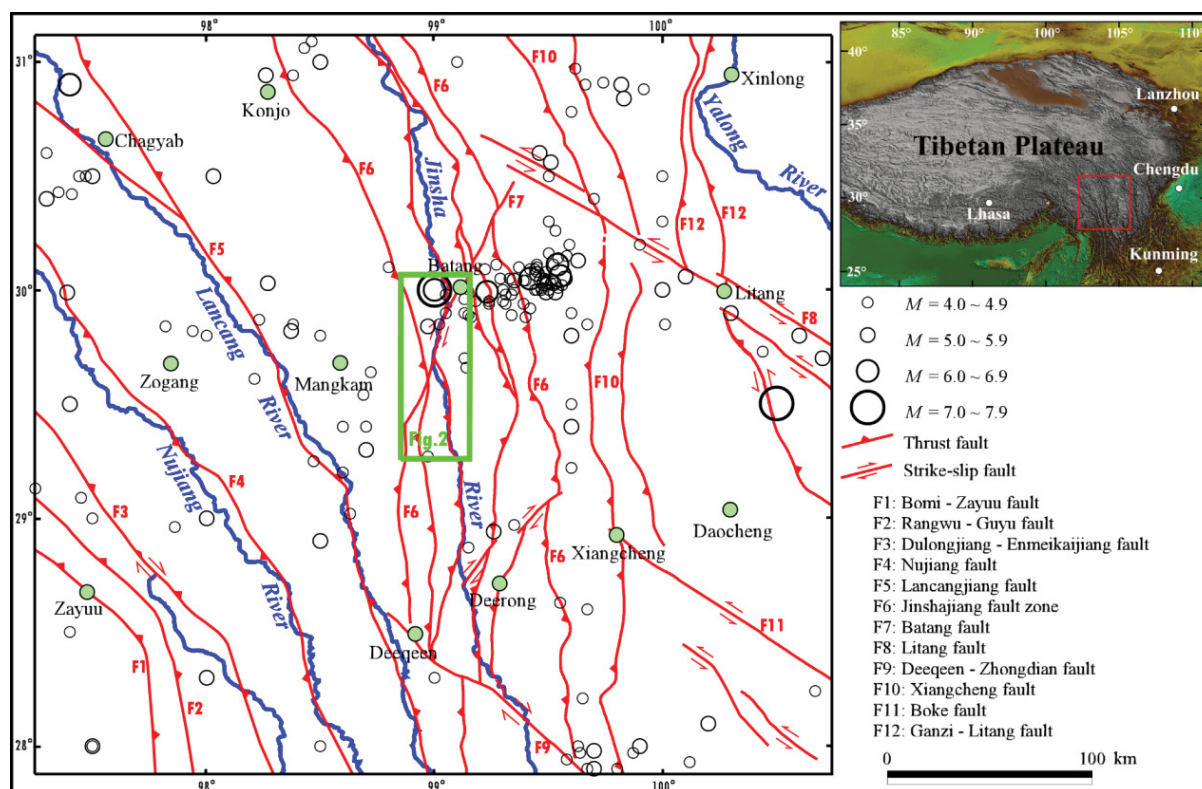
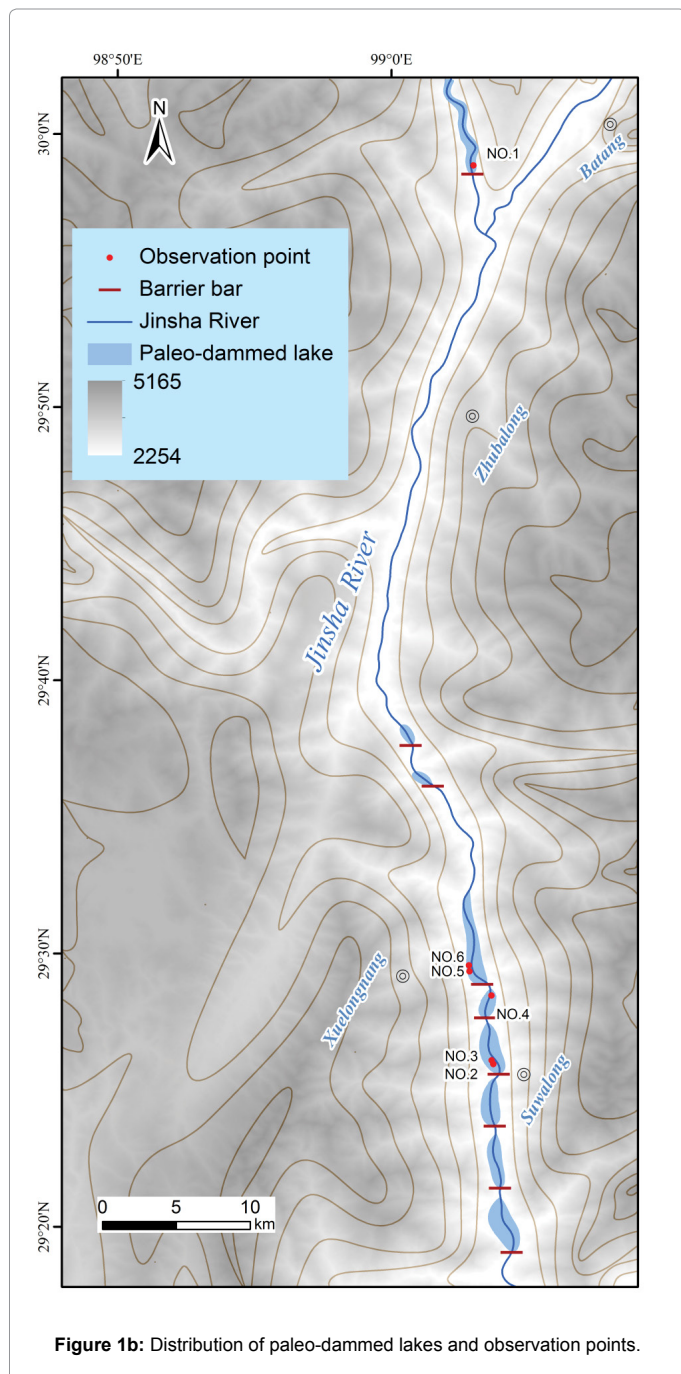


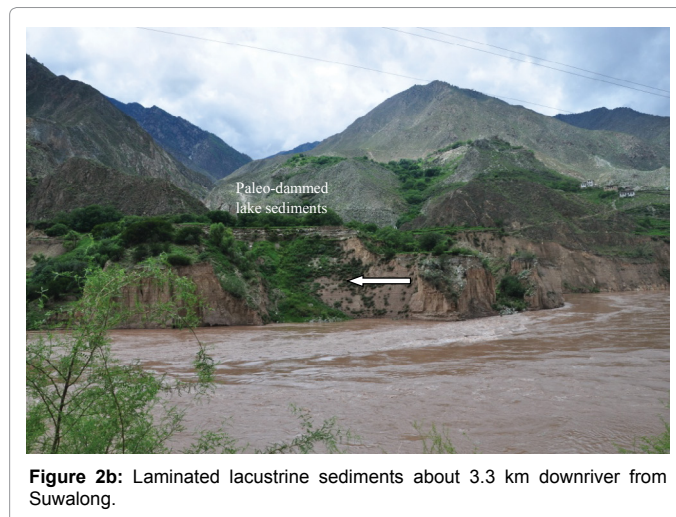
Figure 1a: Map showing the geographic locations of the study site and regional faults.



undeformed. The deformed beddings shaped on the interface of a fine sand layer and the underlying clayey silt layer. The deformation appears that the fine sand was curled by the circumambient clayey silt, just like the shape of a fold (Figure 4b). The convoluted layers are folded with varying amplitude, and the inclination of the axial planes of these folds varies from vertical to near horizontal.

Ball-and-pillow structures

Ball-and-pillow structures had developed in the lacustrine sediment layers at the downstream side at distance of about 50 and 10 m from the Suwalong landslide, respectively (Figures 4a and 5). The composition of the two sedimentary layers is clayey silt layers with a thin layer of



Observation point no.	Altitude (m)	Characteristics of deformation	Corresponding figures
1	2472	Deformed layers	Figures 3a and b
2	2352	Convoluted layers	Figures 4a and b
3	2352	Ball-and-pillow structures	Figure 5
4	2377	Recumbent lamination	Figure 6a and b
5	2392	Water-escape structures	Figure 7a and b
6	2393	Small-scale landslide	Figure 8a and b

Table 1: Location, altitude and characteristics of soft-deformation structures in Batang area.

gray fine sand in the center, and the elevation of each corresponding layer of the two sediments is almost the same.

The deformed beddings shaped distinctly on the interface of a fine sand layer and the underlying clayey silt layer at the lower part of exposed lacustrine sediments (Figure 4a). The thickness of the deformation layer is about 0.8 meter. The deformed layers are folded distinctly with varying amplitude, and the inclination of the axial planes of these folds varies from vertical to near horizontal.

The composition of the sedimentary layer is clayey silt layers with a



Figure 3: Folded layers.
(a) Photograph of laminated lacustrine sediments and two small scale normal faults.



Figure 3b: Close-up of panel.

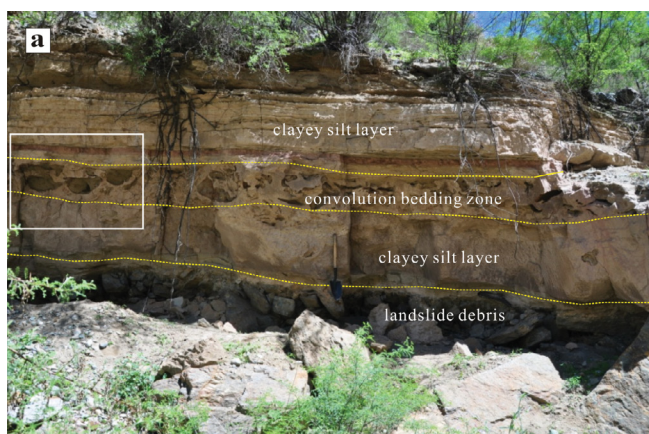


Figure 4: Convoluted layers.
(a) Photograph showing convoluted layers, Note the folding in clayey silt dominated convoluted layers.

thin layer of gray fine sand in the center. In the ball-and-pillow structure (Figure 5), it occurred in the centre of the clayey silt layer underneath (Figures 4b and 5). The gray fine sand appears to have fallen into the

underlying clayey silt layer, and possesses a spherical or pillow-like shape with a maximum size of ~30 cm. The ball-and pillow structures show a gradual upward increase in the extent of deformation, and its overlying clayey silt is undeformed.

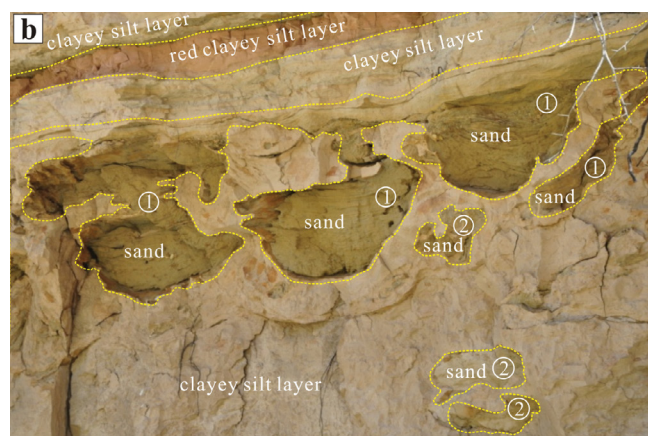


Figure 4b: Close-up of panel.

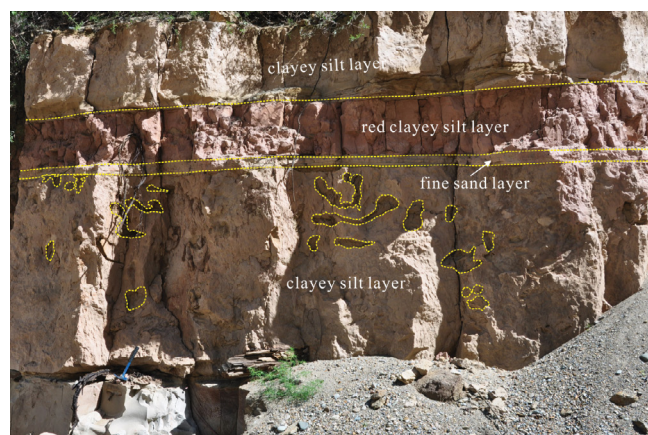


Figure 5: Photograph showing the ball-and-pillow structures.

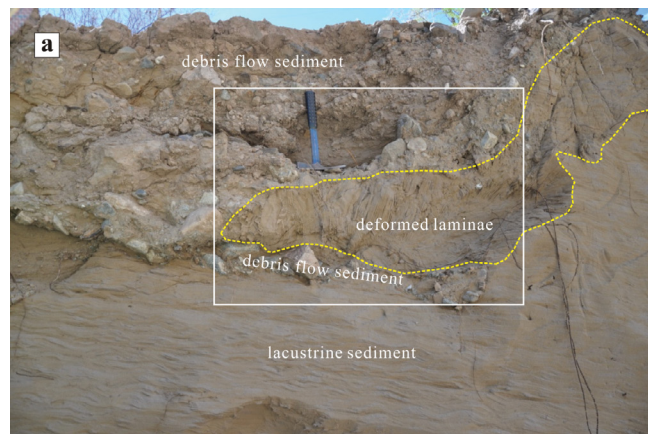


Figure 6: Recumbent lamination.
(a) Photograph showing the folds and broken laminae in silt sand layers.

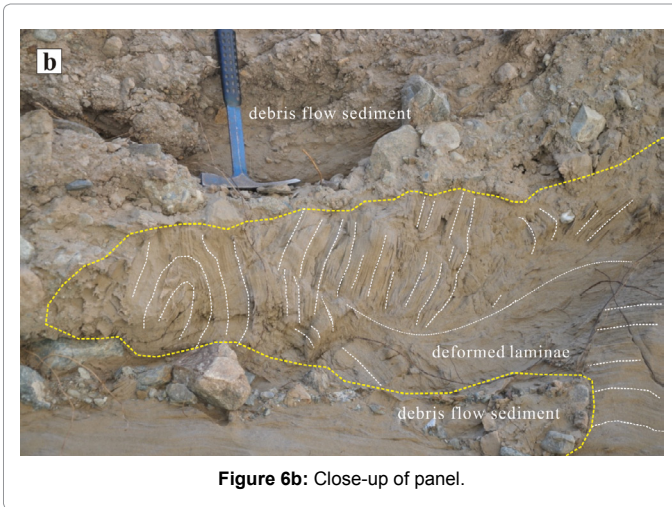


Figure 6b: Close-up of panel.

Recumbent lamination

A 250 cm thick lake sediment with nearly horizontal bedding exposed on the gentle slope terrain. The lake sediment consists of yellow silt sand. At the N side of the upper lake sediment layer, a ~100 cm thick debris-flow sediment layer developed, consisting of gravels, sands and clays. The lake sediment near the bottom or right side of the debris-flow body underwent distinct deformation, characterized by small-scale folds and recumbent laminae (Figures 6a and 7b).

Water-escape structures

Continuous step-like lacustrine successions are well developed at the upstream side of the Xuelongnang paleo-landslide dam along the Jinsha river valley. A 25 cm thick SSD layer occurred in the bottom part of exposed lacustrine sediments, which is characterized by the presence of curvilinear laminae, and mixing of clastics draped by broken silty-clay laminae (Figures 7a and 7b). The mixed clastics consisting in coarse sands and gravels were also shown as inclined or upright dykes. The silty-clay layer is underlied by a 20 cm thick brownish or yellow fine sand horizon. The material of the mixed clastics appears to originate from the underlying sand horizon.

Small-scale landslide

These affect the laminated silty-clay lake sediment layers with a very gentle dip angle (~2°), and reach a maximum thickness of about 120 cm (Figures 8a and 8b). Slump beds are mainly represented by slide structures. In more detail, the deformation features show asymmetrical folds, slide surfaces or disorderly bedding. In certain places some gravels seem to fall randomly into the tension fissures of the deformed sediment. The base of the laminated sediment layer in this profile is undeformed.

Interpretation of Deformation Structures

The presence of discrete deformation layers within the planar beds indicates episodic disturbance during the sedimentation process, which can be triggered by sediment loading, storm-currents, water waves, glaciation, rapid sedimentation or earthquakes [10,16,38-40]. Therefore, in order to identify the origin of the soft-sediment deformation structures (SSDS), some approaches such as criteria-based and trigger-based approaches are adopted to analyze SSDS [25,28,38].

Many studies have investigated the differences between seismic

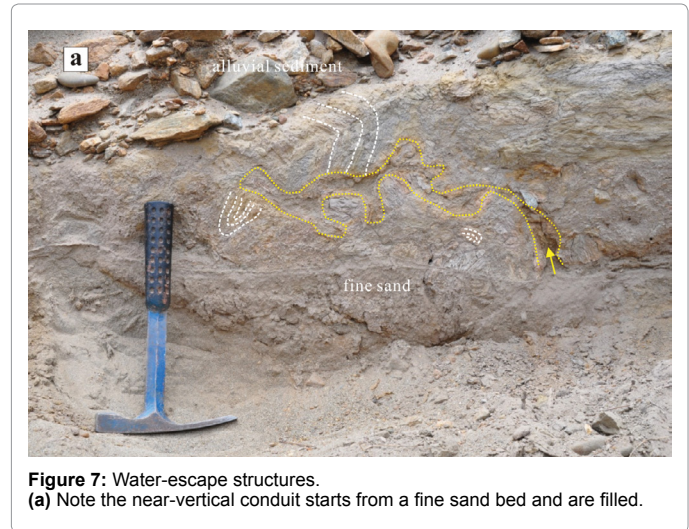


Figure 7: Water-escape structures. (a) Note the near-vertical conduit starts from a fine sand bed and are filled.

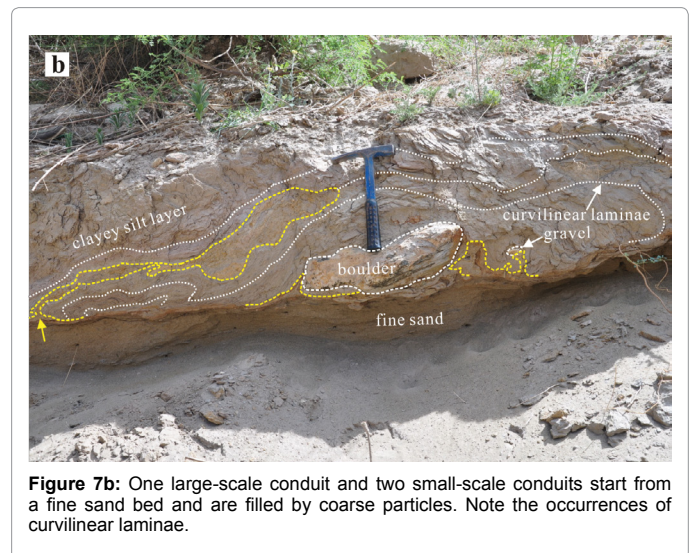


Figure 7b: One large-scale conduit and two small-scale conduits start from a fine sand bed and are filled by coarse particles. Note the occurrences of curvilinear laminae.

and non-seismic deformation structures [10,27,28,30,41,42,55]. In particular, to infer a probable seismic origin, it is necessary to exclude the influence of sedimentary processes on the unconsolidated sediments [26]. In lacustrine successions, this interpretative phase maybe easy as hydrodynamic and sedimentary processes, which are capable of inducing similar soft-sediment deformation structures, are generally absent [43].

The two small-scale normal faults accompanied by clear folding are associated with clayey-silt layers (Figure 3a). The faults are genetically related to earthquakes and are not caused by slope instability, as evidenced by the NW trending dip, which is against the slope of the exposed lake sediments.

The large-scale convoluted layers, folded in different directions, suggest that the deformation occurred at the sediment-water interface, most likely due to the shear produced by the back and forth movement of water over the water saturated laminae during an earthquake (Figure 4a). The origin of similar structures in lacustrine deposits has been attributed to an elastic-plastic response of sediment to shear-stress caused by the back and forth movement of water [15,44].

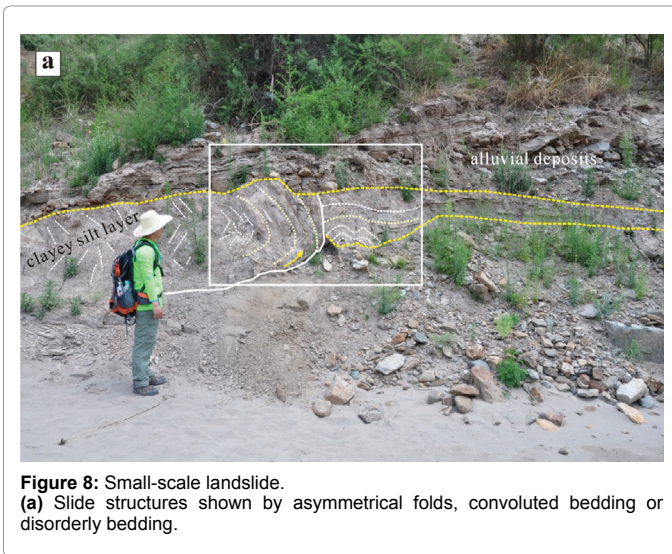


Figure 8: Small-scale landslide. (a) Slide structures shown by asymmetrical folds, convoluted bedding or disorderly bedding.

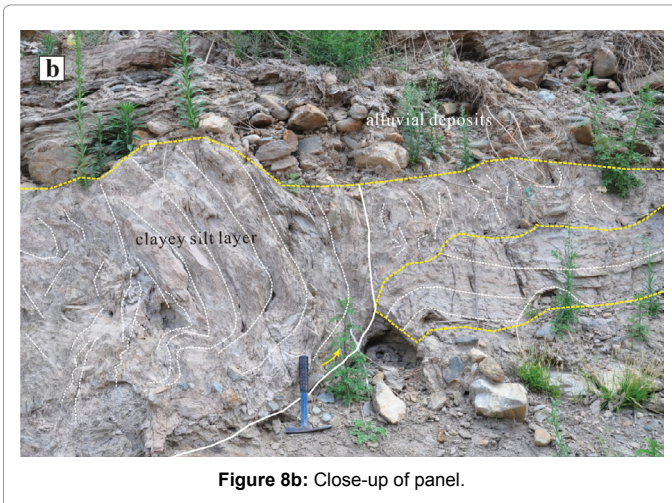


Figure 8b: Close-up of panel.

The ball-and-pillow structures (Figure 5) is a type of load structure, and may form as a consequence of loading of a denser sand layer over a less dense clayey silt layer during earthquake induced liquefaction, so that fine sands would fall into the clayey silt layer in a pillow or globular shape [45]. It could not have possibly been produced by the liquefaction of collapse, as there were no large-scale colluvial deposits in its surrounding area. In addition, the upper and underneath sedimentary layers have horizontal bedding and did not generate lateral deformation or slip surface. The characteristics of soft-sediment deformation show a gradual upward increase in the extent of deformation, also indicating the fact that these structures are most possibly caused by seismic liquefaction [46].

The deformed lamination forms in response to shearing by debris flows. The local deformed lamination only occurred at the bottom or one side of the debris-flow sediments (Figure 6). The relationship between debris-flow facies and the occurrence of deformed lamination reveal that the trigger was flow turbulence in origin. The cohesive and silt sand sediments deform in a plastic or brittle manner [47-50].

The large-scale water-escape structures are associated with the fine-sand horizons (Figures 7a and 7b). Due to the high permeability, these

features are produced by earthquake induced elevated fluid pressure. This pressure is released through the upward flow of fluid, liquefaction and fluidization [20,24,30,33,40] Liquefied and fluidized sediments deform as a viscous fluid. The surrounding cohesive materials behave in a plastic or brittle manner (folded or broken laminae) [28].

Small-scale landslide structures are induced by a mainly lateral driving-force system, due to the presence of a slope. In low-angle slopes deformation begins only after a drastic reduction of the shear strength of the sediments [28]. The behavior is plastic. The facies analysis performed on this succession shows that deformation occurred in a more or less flat depocentral area. We interpret the landslide structures as being seismically-induced (Figure 8a and 8b).

Finally, the presence of more than one type of SSDS, shallow lake depths and geological setting with frequent earthquakes indicates that the genesis of these features is chiefly due to paleo-seismic events [51].

Discussion and Conclusions

On the southeastern margin of the Tibetan Plateau, mass movement occurs frequently and the surface erosion rate is high, thus young strata are rarely preserved. Many landslide-dammed lakes are developed within deep valleys at the southeastern margin of the Tibetan Plateau. In the Batang-Zhongza reaches, based on geomorphological investigation, chronology dating and tectonic setting analysis, the landslides which had formed the landslide-dammed lakes are suggested to be due to multi-period paleo-earthquakes occurring during the Holocene [8,37]. However, direct evidence for the existence of paleo-earthquakes in this area remains absent. The soft-sediment deformation structures related to earthquakes provide an opportunity to better understand the history of seismicity in the Batang area, southeastern Tibet (Table 1).

Our study reveals the widespread development of soft-sediment deformation structures in the Batang paleo-dammed lacustrine sediments. These deformation structures include small-scale normal faults, convoluted layers, ball-and-pillow structures, deformed lamination, water-escape structures, and small-scale slump.

Earthquakes commonly trigger sediment mobilization phenomena, particularly liquefaction and fluidization [36] and soft-sediment structures have commonly been associated with a seismic trigger. However, many other natural agents and processes can act as triggers, including waves, floods, sliding and slumping, rapid loading, bioturbation, cryoturbation, glacial drag, and groundwater movements [39,49]. In general, it is common to adopt contrasting approaches to infer a seismic or non-seismic trigger, based respectively on comparison with a set of established criteria or an assessment of all possible triggers [46].

Combining the assessment of depositional facies, potential triggers, paleoenvironmental context, and available criteria, we may conclude that the trigger agents of the deformation in the Batang area were most likely earthquakes, slides, and debris flows. The seismically-induced soft-sediment deformation structures provide new substantial evidence for the existence of active tectonics and paleo-earthquakes in this area during the Holocene [52-54].

Acknowledgments

The study is supported by the National Natural Science Foundation of China (grants 41571012, 41230743), the Open Research Fund of State Key Laboratory of Simulation and Regulation of Water Cycle in River basin (grant IWHR-SKL-201507), and the Fundamental Research Funds for the Central Universities (grant 2652015060).

References

1. Alsop G, Marco S (2011) Soft-sediment deformation within seismogenic slumps of the Dead Sea Basin. *J Struct Geol* 33: 433–457.
2. Alsop G, Marco S (2012) Tsunami and seiche-triggered deformation within offshore sediments. *Sed Geol* 261: 90–107.
3. Allen JRL (1982) *Sedimentary structures: Their character and physical basis*. Elsevier 2: 663.
4. Becker A, Colin A, Davenport CA, Giardini D (2002) Palaeoseismicity studies on end-Pleistocene and Holocene lake deposits around Basle, Switzerland. *J Int Geophys* 149: 659–678.
5. Ben-Menahem A (1976) Dating of historical earthquakes by mud profiles of lake-bottom sediments. *Nature* 262: 200–202.
6. Chan MA, Bruhn RL (2014) Dynamic liquefaction of Jurassic sand dunes: Processes, origins, and implications. *Earth Surf Proc Land* 39: 1478–1491.
7. Chen J, Dai FC, Lv TY, Cui ZJ (2013) Holocene landslide-dammed lake deposits in the Upper Jinsha River, SE Tibetan Plateau and their ages. *Quat Int J* 298: 107–113.
8. Chen J, Lee HS (2013) Soft-sediment deformation structures in Cambrian siliciclastic and carbonate storm deposits (Shandong Province, China): Differential liquefaction and fluidization triggered by storm-wave loading. *Sed Geol* 288: 81–94.
9. Conti S, Fontana D, Gubertini A, Sighinolfi G, Tateo F, et al. (2004) Multidisciplinary study of middle Miocene seep-carbonates from the northern Apennine foredeep (Italy). *Sed Geol* 169: 1–2, 1–19.
10. Cui ZJ (2013) *Diamicton and Environment*. Science and Technology Press of Hebei Province, Hebei pp. 584–596
11. Douillet GA, Taisne B, Tsang-Hine-Sun E, Müller SK, Kueppers U, et al. (2015) Syn-eruptive, soft-sediment deformation of deposits from dilute pyroclastic density current: triggers from granular shear, dynamic pore pressure, ballistic impacts and shock waves. *Solid Earth* 6: 553–572.
12. Frey SE, Gingras MK, Dashtgard SE (2009) Experimental studies of gas-escape and water-escape structures: mechanisms and morphologies. *Sed Res J* 79: 808–816.
13. He B, Qiao X, Zhang Y, Tian H, Cai Z, et al. (2015) Soft-sediment deformation structures in the Cretaceous Zhucheng depression, Shandong Province, East China: Their character, deformation timing and tectonic implications. *Asian Earth Sci J* 110: 101–122.
14. Hempton MR, Dewey JF (1983) Earthquake-induced deformational structures in young lacustrine sediments, East Anatolian Fault, southeast Turkey. *Tectonophysics* 98: 7–14.
15. Hibsich C, Alvarado A, Yepes H, Perez VH, Sebrier M, et al. (1997) Holocene liquefaction and soft-sediment deformation in Quito (Ecuador): A paleoseismic history recorded in lacustrine sediments. *Geodynamics J* 24: 259–280.
16. Jones AP, Omoto K (2000) Toward establishing criteria for identifying trigger mechanism for soft-sediment deformation: A case study of Late Pleistocene lacustrine sand and clays, Onkobe and Nakayamadaira. *Sedimentology* 47: 1211–1226.
17. Karlin, RE, Abella SEB (1992) Paleoseismicity in the Puget Sound Region recorded in sediments from lake Washington, U.S.A. *Science* 258: 1617–1619.
18. Knight J (2015) Ductile and brittle styles of subglacial sediment deformation: An example from western Ireland. *Sedimentary Geol* 318: 85–96.
19. Long W, Chen J, Wang PF, Xu C, Liu H, et al. (2015) Formation mechanism and back analysis of Paleoseismic parameters of the Temi large-scale ancient landslide in the upper Jinsha River. *Seismological Res J* 38: 568–575.
20. Lowe DR (1975) Water escape structures in coarse-grained sediments. *Sedimentology* 22: 157–204.
21. Lowe DR (1976) Subaqueous liquefied and fluidized sediment flows and their deposits. *Sedimentology* 23: 285–308.
22. McCaillin J (1996) *Paleoseismology*. Academic Press, New York.
23. Migowski C, Agnon A, Bookman R, Negendank JFW, Stein M (2004) Recurrence pattern of Holocene earthquakes along the Dead Sea transform revealed by varve-counting and radiocarbon dating of lacustrine sediments. *Earth Planet Sci Lett* 222: 301–314.
24. Mills PC (1983) Genesis and diagnostic value of soft-sediment deformation structures—a review. *Sedimentary Geol* 35: 83–104.
25. Montenat C, Barrier P, Ott d'Estevou P, Hibsich C (2007) Seismites: An attempt at critical analysis and classification. *Sedimentary Geol* 196: 5–30.
26. Moretti M (2000) Soft-sediment deformation structures interpreted as seismites in middle-late Pleistocene aeolian deposits (Apulian foreland, southern Italy). *Sediment Geol* 135: 167–179.
27. Moretti M, Soria JM, Alfaro P, Walsh N (2001) Asymmetrical soft-sediment deformation structures triggered by rapid sedimentation in turbiditic deposits. *Facies* 44: 283–294.
28. Moretti M, Sabato L (2007) Recognition of trigger mechanisms for soft-sediment deformation in the Pleistocene lacustrine deposits of the Sant'Arcangelo Basin (Southern Italy): Seismic shock vs. overloading. *Sedimentary Geol* 196: 31–45.
29. Nichols RJ, Sparks RSJ, Wilson CJN (1994) Experimental studies of the fluidization of layered sediments and the formation of fluid escape structures. *Sedimentology* 41: 233–253.
30. Obermeier SF (1996) Use of liquefaction-induced features for paleoseismic analysis—an overview of how seismic liquefaction features can be distinguished from other features and how their regional distribution and properties of source sediment can be used to infer the location and strength of Holocene paleo-earthquakes. *Engineering Geol* 44: 1–76.
31. Owen G (1987) Deformation processes in unconsolidated sands. In: Jones ME, Preston RMF (Eds), *Deformation of Sediments and Sedimentary Rocks*. Geological Society, London Spec Publ 29: 11–24.
32. Seed HB (1979) Soil liquefaction and cyclic mobility evaluation for level ground during earthquakes. *Proceedings of the American Society of Civil Engineers, Geotechnical Eng J* 105: 201–255.
33. Owen G (1996) Experimental soft-sediment deformation: structures formed by the liquefaction of unconsolidated sands and some ancient examples. *Sedimentology* 43: 279–293.
34. Qiao X, Song T, Gao L, Li H, Peng Y, et al. (2006) *Seismic Records in Strata (Ancient Earthquake)*. Geological Publishing House, Beijing. pp. 1–263.
35. Xu XW, Zhang PZ, Wen XZ, Qin ZL, Chen GH, et al. (2005) Features of active tectonics and recurrence behaviors of strong earthquakes in the western Sichuan Province and its adjacent regions. *Seismol Geol* 27: 446–461.
36. Wu XG, Cai CX (1992) The neotectonic activity along the central segment of Jinshajiang Fault zone and the epicentral determination of Batang M 6.5 earthquake. *J Seismol Res* 15: 401–410.
37. Wang PF, Chen J, Dai FC, Long W, Xu C, et al. (2014) Chronology of relict lake deposits around the Suwalong paleo-landslide in the upper Jinsha River, SE Tibetan Plateau: Implications to Holocene tectonic perturbations. *Geomorphology* 217: 193–203.
38. Rossetti DF (1999) Soft-sediment deformation structures in late Albian to Cenomanian deposits, Sao Luís Basin, northern Brazil: Evidence for paleoseismicity. *Sedimentology* 46: 1065–1081.
39. Owen G, Moretti M (2011a) Identifying triggers for liquefaction-induced soft-sediment deformation in sands. *Sedimentary Geol* 235: 141–147.
40. Rana N, Bhattacharya F, Basavaiah N, Pant RK, Juyal N, et al. (2013) Soft sediment deformation structures and their implications for Late Quaternary seismicity on the South Tibetan Detachment System, Central Himalaya (Uttarakhand), India. *Tectonophysics* 592: 165–174.
41. Seilacher A (1984) Sedimentary structures tentatively attributed to seismic events. *Marine Geol* 55: 1–12.
42. Wheeler RL (2002) Distinguishing seismic from nonseismic soft sediment structures; criteria from seismic-hazard analysis. In: Etensohn, F.R., Rast, N., Brett, C.E. (Eds.), *Ancient Seismites*: Geological Society of America Special Paper 359, pp. 1–11.
43. Sims JD (1973) Earthquake-induced structures in sediments of Van Norman Lake, San Fernando, California. *Science* 182: 161–163.
44. Rodríguez-Pascua MA, Calvo JP, De Vicente G, Gómez-Gras D (2000) Soft-sediment deformation structures interpreted as seismites in lacustrine sediments of the Prebetic Zone, SE Spain, and their potential use as indicators of earthquake magnitudes during the Late Miocene. *Sedimentary Geol* 135: 117–135.

45. Qiao X, Li H (2008) Pillow, ball-and-pillow structures: paleo-seismic records within strata. *Geol Rev* 54: 721–730.
46. Owen G, Moretti M, Alfaro P (2011b) Recognising triggers for soft-sediment deformation: Current understanding and future directions. *Sedimentary Geol* 235: 133–140.
47. Rossetti DF, Góes AM (2000) Deciphering the sedimentological imprint of paleoseismic events: An example from the Aptian Codó Formation, northern Brazil. *Sedimentary Geol* 135: 137–156.
48. Santos MGM, Almeida RP, Mountney NP, Fragoso-Cesar ARS (2012) Seismites as a tool in the palaeoenvironmental reconstruction of fluvial deposits: The Cambrian Guarda Velha Formation, southern Brazil. *Sedimentary Geol* 277–278: 52–60.
49. Sims JD (1975) Determining earthquake recurrence intervals from deformational structures in young lacustrine sediments. *Tectonophysics* 29: 141–152.
50. Singh S, Jain AK (2007) Liquefaction and fluidization of lacustrine deposits from Lahaul-Spiti and Ladakh Himalaya: geological evidences of paleoseismicity along active fault zone. *Sedimentary Geol* 196: 47–57.
51. Schnellmann M, Anselmetti F, Giardini D, McKenzie J (2005) Mass movement-induced fold-and-thrust belt structures in unconsolidated sediments in Lake Lucerne (Switzerland). *Sedimentology* 52/2: 271–289.
52. Van Loon AJ, Brodzikowski K, Zielinski (1995) Shock-induced resuspension deposits from a Pleistocene proglacial lake (Kleszczów Graben, central Poland). *Sedimentary Res* 65: 417–422.
53. Wang P, Zhang B, Qiu WL, Wang JC (2011) Soft-sediment deformation structures from the Diexi paleo-dammed lakes in the upper reaches of the Minjiang River, east Tibet. *Asian Earth Sci J* 40: 865–872.
54. Weidlich O, Bernecker M (2004) Quantification of depositional changes and paleo-seismic activities from laminated sediments using outcrop data. *Sediment Geol* 166: 11–20.